

## Article

# Biogeofilter with Hydrothermal Treated Stevensite Clay and Laccase Enzymes for Retention and Degradation of Tetracycline

Adrien Saphy<sup>1,2</sup>, María Tijero<sup>1</sup>, Carlos García-Delgado<sup>1</sup> , Almudena Ortega<sup>1</sup>, Sergio Zamora<sup>3</sup>, Ana Isabel Ruiz<sup>1</sup>, Enrique Eymar<sup>3</sup>, Jaime Cuevas<sup>1</sup>  and Raúl Fernández<sup>1,\*</sup> 

<sup>1</sup> Departamento de Geología y Geoquímica, Universidad Autónoma de Madrid, 28049 Madrid, Spain

<sup>2</sup> Ecole et Observatoire des Sciences de la Terre, Université de Strasbourg, 67084 Strasbourg, France

<sup>3</sup> Departamento de Química Agrícola y Bromatología, Universidad Autónoma de Madrid, 28049 Madrid, Spain

\* Correspondence: raul.fernandez@uam.es

**Abstract:** The concentration of antibiotics in surface water is an issue of high concern. The present study aims to manufacture and evaluate a biogeofilter, with stevensite clay and enzymes immobilized on it, for the adsorption and degradation of tetracycline-based antibiotics. To retain the small particle aggregates of the clay in the filter, a hydrothermal treatment was applied to the stevensite, prior to compaction in pellets and its insertion into a cylindrical cell, mixed with sand. The structure of the pellets avoids the loss of the clay material during the fluid transport through the porous medium. Several temperature treatments were applied to the pellets, but the treatment at 300 °C was revealed as the best option. Laccase enzymes were immobilized on the stevensite surface. Reactive transport experiments of tetracycline solutions were performed through the transport cells. The biogeofilter has a relevant adsorption capacity with a significant degradation factor. By modelling with STANMOD software, the hydrodynamic characteristics of the transport were determined and, therefore, the behaviour of a large-scale filter and transports of low tetracycline concentrations could be predicted. The results obtained are promising for irrigation systems at medium scale, as well as for the perspective of wastewater treatment plants at large scale.

**Keywords:** stevensite; pellets; biogeofilter; antibiotic pollutants; tetracycline; STANMOD



**Citation:** Saphy, A.; Tijero, M.; García-Delgado, C.; Ortega, A.; Zamora, S.; Ruiz, A.I.; Eymar, E.; Cuevas, J.; Fernández, R. Biogeofilter with Hydrothermal Treated Stevensite Clay and Laccase Enzymes for Retention and Degradation of Tetracycline. *Minerals* **2022**, *12*, 1631. <https://doi.org/10.3390/min12121631>

Academic Editors: Juan Antelo and Janos Kristof

Received: 1 November 2022

Accepted: 15 December 2022

Published: 17 December 2022

**Publisher's Note:** MDPI stays neutral with regard to jurisdictional claims in published maps and institutional affiliations.



**Copyright:** © 2022 by the authors. Licensee MDPI, Basel, Switzerland. This article is an open access article distributed under the terms and conditions of the Creative Commons Attribution (CC BY) license (<https://creativecommons.org/licenses/by/4.0/>).

## 1. Introduction

The large extended presence of antibiotics in wastewater and in agricultural products is an issue of high concern due to their persistence and the potential risk for living organisms [1,2]. Antibiotics are only partially digested and absorbed by humans and animals. Approximately half of the antibiotics administered to humans and animals are actively excreted unchanged within 8–24 h after consumption, primarily through urine and feces. The literature reports an incomplete absorption of 20% to 95% of the administered antibiotics, and the production of metabolites, which form after degradation, can be even more toxic than the original compound. The metabolites can accumulate in all habitats, especially surface waters, groundwaters, soils and sediments, through treated or untreated wastewater [2–5].

Conventional wastewater treatment plants (WWTPs) are based on chemical and physical processes, such as filtration, flocculation, coagulation, sedimentation and biological processes that mostly occur on activated sludge [6]. The main historical objective in WWTPs was the removal of solids and the reduction of organic matter. In the last few decades, technology has been implemented to eliminate nutrients, such as nitrates and phosphates, increase the yields in all the processes and, in general, improve the quality of the outflow water and take advantage of the residues, such as the sludge and the produced gas, that could be considered as a resource for different applications. However, for the removal of antibiotics in wastewater effluents and sludges, additional treatments need to be provided

before effluents are discharged to the environment or sludges are used for other purposes, such as agricultural [3].

Various additional treatment technologies have been shown to remove antibiotics from wastewaters, for instance, physical treatments [4], disinfection [7], advanced oxidation [8] and filtration with a permeable material with a high adsorption capacity, such as activated carbon [9]. The use of low-cost materials, such as clays, for adsorption of antibiotics from wastewaters, in addition to other organic and inorganic pollutants, has been extensively studied. Clay-based adsorbents have high adsorption potential, but a significant remaining gap exists between theoretical studies and laboratory-scale experiments, and their real application at industrial scale [10].

Natural clays are mostly composed of clay minerals, in addition to accessory minerals and other possible minor components, such as oxides and organic matter, typically in very minor concentration. In general, they exhibit good properties for adsorption due to their adequate physico-chemical properties: small particle size, high surface area, cation exchange capacity with fast kinetic mechanism and channels or zones to accumulate a high number of molecules [11].

Kaolinite, sepiolite, palygorskite, rectorite, illite and the smectite montmorillonite have been studied as the most promising clay minerals to use for the adsorption of antibiotics [12–15]. However, clay minerals have been demonstrated to be very sensible to external parameters, such as pH, temperature, salinity and competition with other organic compounds [10].

Thiebault et al. [16] showed that the efficiency of a geofilter made of a mixture of sand and montmorillonite requires low clay content and a clay material that provides functional permeability. In their study, they demonstrated that Na-montmorillonite exerted high swelling pressure in the filter, limiting the permeability of the porous media, even at a low clay percentage (5%), whereas a Ca-montmorillonite allowed better percolation.

Stevensite, a 2:1 trioctahedral smectite with an octahedral sheet rich in Mg, is grouped within the Mg-smectite minerals and exhibits additional promising properties. However, it has been less studied because it is found at commercial grade in few places around the world [17]. Mg-clays are frequent and exploited in the Madrid Basin [18]. Such clays have good adsorbing capacities due to cationic exchanges and other molecular interactions. Previous studies [19,20] have shown that the commercial clay Minclear N100<sup>TM</sup>, distributed by Tolsa (Spain) and composed of >90% stevensite ( $\text{Si}_4\text{Al}_{0.4}\text{Fe}_{0.1}\text{Mg}_{2.1}\text{M}^{+0.3}\text{O}_{10}(\text{OH})_2$ , from X-ray fluorescence analysis of Ca-homoionized <2  $\mu\text{m}$  size fraction [21]), <10% illite and dolomite and <1% feldspars and quartz, has excellent properties for TC adsorption, both in batch experiments (static conditions) and in flow-through transport experiments (dynamic conditions), not only at low pH conditions, but also at neutral pH (6–8), which is normally the range of pH of wastewaters in urban WWTPs. However, the nanometric to micrometric size of the clay particles makes them lose out during transport with the mobile solution by colloidal dispersion. Fernández et al. [20] designed their transport experiment by adding to a cylindrical column a mixture of finely grinded silica sand and stevensite in mass ratio 10:1 in order to prevent excessive swelling. Polypropylene filters of 0.45  $\mu\text{m}$  pore size, geotextile filters and porous Teflon filters were added to both sides of the column to maintain the stevensite on site and prevent loss of clay.

In the present work, the stevensite clay material Minclear N100<sup>TM</sup> has been hydrothermally modified over the temperature of reversible dehydration and below the temperature of dehydroxilation with the aim to limit even more colloidal dispersion and swelling. Due to the applied physical treatment, stevensite thin (<2 mm diameter) pellets with centimetric length were obtained with a rigid macroscopic structure.

Similar approaches, such as the work from Polubesova et al. [22] that created a micelle-clay filter made of benzyltrimethylhexadecylammonium (BDMHDA)montmorillonite in a cylindrical column mixed with quartz sand at 100/1 (*w/w*) sand:BDMHDA–clay complex ratio, demonstrated high efficiency for the removal of negatively charged tetracycline and sulfonamide antibiotics from water at pH 8.5 (>90%). Biofilters are also used to reduce the

concentration of antibiotics in water. Ligninolytic enzymes, such as laccase and peroxidase, facilitate the biodegradation of organic pollutants, such as environmentally persistent pharmaceutical pollutants [23]. Laccase enzyme is a non-selective oxidase implied in many degradation processes. The large spectra of organic compounds degradable by laccase can be useful for wastewater treatment, even more so if the enzyme is immobilized on the clay substrate, avoiding its wide spread in the environment.

To study the filtering capacity, transport reactive tests must be conducted. In the present study, the adsorption capacities of the clay have been tested after different hydrothermal treatments with different concentrations of the injected solution, with or without enzyme, in order to find the best performance for the filter.

Reactive transport tests are conducted at the laboratory scale through relatively small filter cells. The perspective of this study is to develop a filter that could be used in WWTPs to reduce the concentration of antibiotics in their effluents. Filters can also be designed in smaller sizes for domestic or agricultural use to remove antibiotics from water before reusing it.

In addition, modelling according to reactive transport equations in porous media have been used to determine the hydrodynamic parameters of the filter, namely the retardation factor and the degradation term. Those two parameters are characteristic of the quality of the filter, such that the higher they are, the better the filtering capacity is. Modelling allows prediction of the application of this filter at different scales.

Most of the experiments have been carried out with tetracycline hydrochloride solution (TC), the most used derivative from tetracycline for veterinary purposes (Figure 1). Tetracycline, even in low concentrations (in the order of 10 ppb), has a selection effect on antibiotic resistance genes [24] and a selection effect on resistant bacteria in our environment. Furthermore, high concentrations of tetracycline are found in many effluents in Europe; for example, concentrations above 100 ppb were found in the final effluents of WWTPs in Ireland, Norway and Portugal [25].

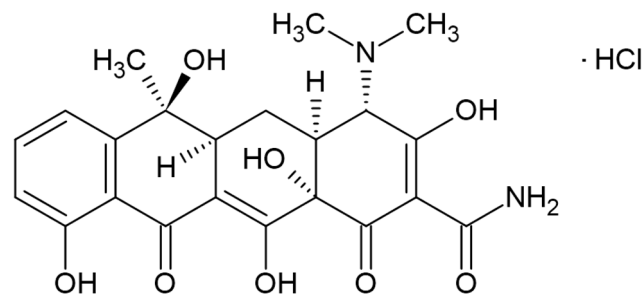


**Figure 1.** TC molecule used in the present study (drawn with ChemSketch Freeware software, version 2021.2.1, ACD/Labs, Toronto, ON, Canada [26]).

Therefore, to adsorb and then degrade the antibiotics, the present study employs a filter based on stevensite clay with immobilized laccase enzymes on it. The main objective of the present research work is to develop such a filter, to determine its characteristics and to carry out laboratory tests on the transport of antibiotics through this filter. The filter must be resistant to colloidal dispersion, must adsorb tetracycline and must degrade the tetracycline in an enzymatic way. The hydrodynamic characteristics, calculated by the STANMOD model, will allow proposing a prediction of the filter behaviour at large scale.

## 2. Materials and Methods

### 2.1. Experiments

#### 2.1.1. Hydrothermal Treatment of the Clays

The stevensite clay was kneaded in presence of deionized water at a solid to liquid ratio = 1 (1 kg:1 L). Then, it was extruded into threads of 2 mm in diameter and dried at atmospheric conditions or in an oven at 60 °C until the humidity decreased from 100 to 30%. As the humidity decreased, the threads began to fracture into smaller aggre-

gates. In a first stage, these aggregates were heated at 200 °C for a week inside a hermetic reactor in order to stabilize them into pellets without deteriorating their cation exchange capacity (CEC).

These pellets were allowed to react with steam, which is known to make smectites lose their swelling capacity [27], maintaining the crystalline structure of smectite unaffected [28].

Thermal treatment at higher temperature (second stage) was performed using the pellets previously treated at 200 °C, heating for 2 h at 300, 400 and 500 °C in melting pots with the objective to compare the physical stability of the pellets and their physico-chemical properties (CEC and BET-specific surface area). Higher physical stability with minimum decrease of CEC and BET was sought. CEC was measured by the Cu-trien method [29], while the BET-specific surface area was determined by N<sub>2</sub> adsorption in a Micromeritics Gemini V analyzer (Norcross, GA, USA). The detailed screening of physico-chemical properties of these materials was provided by Tijero [21]. However, only the results of treatments relevant for the present study are reproduced here.

### 2.1.2. Transport Experiments

The transport tests were carried out through cylinders of 1 cm radius by 2 cm height bounded by two sintered stainless steel porous filters.

A 1:1 mixture of clay pellets:sand was used, filling the inner dimensions of the cylinder. The ideal total mass of this mixture is 9 g, but the real mass depends on manual compaction and the distribution of particles in the cylinder. This proportion allows the sand to simply decrease the porosity of the medium and, therefore, decrease the velocity of the transport through the cell. The cells are mounted vertically, supported by a tripod and clamp that are connected to the top and bottom of the transport system. A solution of our choice can be injected, with a flow imposed by a pump from the lower part. All experiments were conducted with a constant injected solution flow of 1 mL min<sup>-1</sup>. At the upper part, there is a system for collecting the outflow solution (Figure 2). The outflow solution must be collected at regular time or volume intervals.

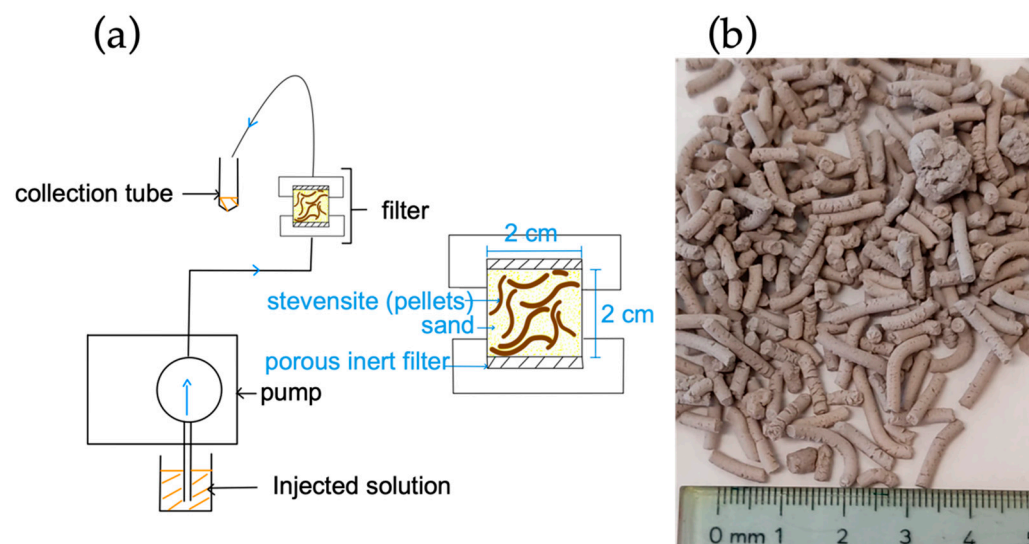


**Figure 2.** (a) Scheme of the experimental set-up of reactive transport experiments; (b) aspect of the stevensite pellets.

Most of the transport tests were performed dissolving 1 g of TC in 1 L of water at an initial pH = 2.3, without any other matrix to fix the ionic strength. Under these conditions, TC remains in its cationic state. However, it was necessary to carry out a first non-reactive transport to determine the hydrodynamic parameters. For that, a sodium nitrate solution 1 M was used. Specific tests were carried out with other organic molecules, an anion (eriochrome cyanine R) and a neutral polar molecule (4-nitrophenol). For the desorption

step, a concentrated solution of magnesium nitrate 1 M was used. All experiments were performed at room temperature

### 2.1.3. Immobilization of Laccase

Commercial laccase from *Aspergillus* sp. (Sigma-Aldrich, Burlington, MA, USA) was used for the immobilization on stevensite. The laccase immobilization was tested with and without partial purification. The partial purification of laccase was based on ammonium sulphate precipitation (90% saturation) and subsequent centrifugation at 10,000 rpm, 2 h. The precipitate was dissolved in potassium phosphate buffer 0.1 M pH 7.0, passed through a PD-10 desalting column (GE Healthcare) and then used for the laccase immobilization process. Laccase activity was determined spectrophotometrically by following the oxidation of 2,6-dimethoxyphenol in 50 mM sodium acetate buffer (pH 5.0) at 477 nm ( $\epsilon = 14,600 \text{ mol L}^{-1} \text{ cm}^{-1}$ ). One international unit (IU) was defined as the amount of enzyme producing 1.0  $\mu\text{mol}$  of product per minute under the assay conditions [30].

A cross-link technique was used with glutaraldehyde, which is one of the easiest techniques of enzyme immobilization [31]. For 1 g of clay, 40 mL of enzyme solution (300 IU) were added in phosphate buffer pH 7.0 containing 0.8 mL of glutaraldehyde. The mixture was kept under agitation for 24 h at 4 °C. Then, the stevensite clay—immobilized laccase pellets were washed with the buffer solution after no laccase activity was detected in supernatant.

To increase the degradation kinetics, syringaldehyde (a redox intermediate) was used. Once oxidized by laccase, a radical form of syringaldehyde is produced, with capacity to degrade tetracycline [30].

### 2.1.4. Analyses of Solutes

Ions concentrations, such as nitrate when used as a single ion solution (dissolved  $\text{NaNO}_3$ ), were indirectly measured by electrical conductivity, using a Metrohm 712 conductometer. A calibration curve between concentration and conductivity is required beforehand, but the method is fast and allows the live determinations during the transport experiments.

The analysis of TC was performed by high-performance liquid chromatography coupled to a photodiode array detector (HPLC-DAD) in an apparatus consisting of an e2695 Separation Module coupled with a Waters 2998 HPLC-DAD (Waters, Milford, MA, USA). Chromatographic separation of TC was achieved with a Phenomenex Luna C18(2) (150 mm  $\times$  4.6 mm; particle size 5  $\mu\text{m}$ ) column, using a gradient elution program with trifluoroacetic acid 10 mM (TFA) and acetonitrile (ACN) at a flow rate of 0.8 mL  $\text{min}^{-1}$ . The gradient elution program was 0–1 min: 80% TFA and 20% ACN, then a linear gradient elution from 20% ACN at 1 min to 30% acetonitrile at 4 min, followed by isocratic elution for 3 min. The column temperature was set at 40 °C. The injection volume was 10  $\mu\text{L}$ . The elution profiles were monitored at 270 nm. TC was identified based on both UV spectra and retention time of commercially available standard (Sigma-Aldrich).

## 2.2. Model

### 2.2.1. Reactive Transport Model

To interpret the transport tests, a reactive transport model was used. Due to the dimensions of the transport cell, the model can be approached by a 1-dimension problem. It is theoretically in the case of a simple advection-dispersion transport. The reactive transport follows the convective-dispersive transport Equation (1) [32]:

$$R \frac{\partial c}{\partial t} = D \frac{\partial^2 c}{\partial x^2} - v \frac{\partial c}{\partial x} \quad (1)$$

where  $R$  = retardation factor;  $D$  = dispersion coefficient;  $v$  = porewater velocity;  $x$  = coordinate parallel to flow;  $c$  = concentration of the solute; and  $t$  = time.

Ogata and Banks [33] proposed an analytical solution to the Equation (1) in porous media, formulated by Equation (2):

$$\frac{c(x,t)}{c_0} = \frac{1}{2} \left( \operatorname{erfc} \left( \frac{x-ut}{2\sqrt{Dt}} \right) + \exp \left( \frac{ux}{D} \right) * \operatorname{erfc} \left( \frac{x+ut}{2\sqrt{Dt}} \right) \right) \quad (2)$$

where  $u$  = average velocity of fluid or superficial velocity/porosity of medium. In the case with enzymes immobilized on clays, the enzymatic degradation is expected to affect transport. Therefore, it is necessary to add a degradation term to the equation.

As the reaction mechanism of tetracycline degradation by laccase is rather complex, especially due to the redox intermediate used, a reaction following first order kinetics will be assumed (Equation (3)).

$$R \frac{\partial c}{\partial t} = D \frac{\partial^2 c}{\partial x^2} - v \frac{\partial c}{\partial x} - \mu c \quad (3)$$

where  $\mu$  = degradation factor.

The analytical solution of the latter equation was recently reported for a contaminant transport through a vertical cut-off wall and aquifer system [34].

### 2.2.2. Computing with STANMOD

The reactive transport models have been performed in the present study by means of the STANMOD software (version 2.08, PC-progress, Prague, Czech Republic). STANMOD is used for the simulation of reactive transport through porous media. It is based on the Van Genuchten equations [35]. Solving them, a flow can be simulated, taking into account characteristic parameters of the medium, such as dispersion, porosity, pore water velocity, etc., but also parameters of the reactant, such as the retardation and degradation factors that may be applicable in the case of the use of enzymes.

There are several methods that can be used within the STANMOD software. For the present study, the inverse method CXTFIT has been used to estimate the transport parameters [36–38]. The breakthrough curve obtained by experiments is fitted with the analytical solution solving the theoretical equations, leaving one degree of freedom.

For the sake of clarity, representations of breakthrough curves are shown as a function of time in the present study, allowing direct comparison of experimental data with the models obtained with STANMOD. The time scale could be transformed to pore volume, considering the injected solution flow of 1 mL/min and assuming an initial constant pore volume in the filter of 2.8 cm<sup>3</sup>.

### 2.2.3. Calculation of Hydrodynamic Parameters

When fitting the data, several different parameter combinations can lead to the same result. Therefore, approximation by other models allows testing the reliability of the present modelling.

The moment method is based on an approximation of the area under the concentration-time curve to estimate the residence time of the molecule in the filter.

A retardation factor approximation is sometimes used, indicating that  $R$  is equal to the ratio of the velocity of the non-reactive transport by the velocity of the reactive transport.

Finally, some approximations use the adsorption isotherm model to approximate the retardation factor. The determination of the retardation factor  $R$  with the Freundlich isotherm is explained by Equation (4) [39]:

$$R = 1 + \frac{1-n}{n} \rho K C_{eq}^{N-1} \quad (4)$$

where  $n$  = porosity;  $K$  and  $N$  = Freundlich constant and exponent;  $\rho$  = bulk density; and  $C_{eq}$  = concentration at equilibrium.

In order to compare the different retardation factors, it is necessary that they were calculated with the same method, and to better compare them, the normalized  $R$  was calculated as described by Equation (5):

$$R_{\text{normalized}} = \frac{R}{m_{\text{clay}} \times C_{\text{injected}}} \quad (5)$$

Finally, to distinguish the influence of the degradation and the other mechanisms, such as sorption or other reactions, the ratio of the area under the breakthrough curve of the sample with the enzyme over the one with the sample without enzyme have been calculated by Equation (6):

$$\% \text{ degraded} = \left( 1 - \frac{A_{\text{with enzyme}}}{A_{\text{without}}} \right) \times 100 \quad (6)$$

### 3. Results

#### 3.1. CEC and Specific Surface Area of Pellets

The CEC and the BET-specific surface area were determined in the original clay and in all hydrothermally treated samples with the objective to predict the adsorption capacities of the stevensite pellets (Figure 3).

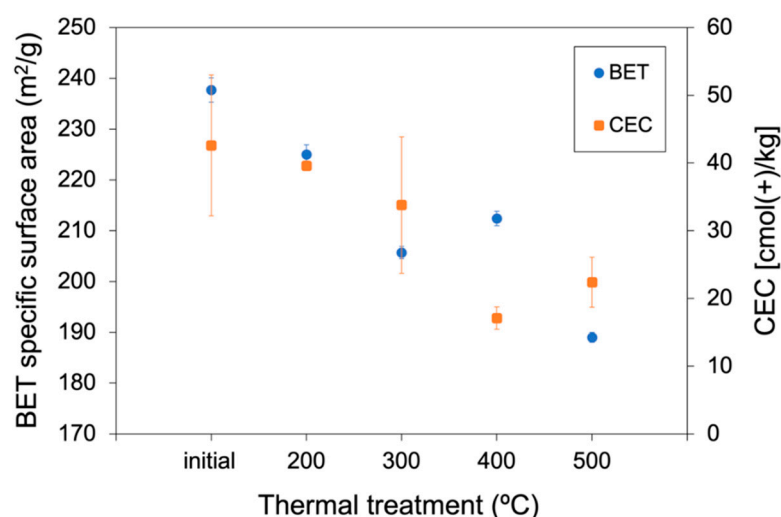


**Figure 3.** CEC and specific surface area of the initial stevensite (before any hydrothermal treatment) and thermally treated samples at 200, 300, 400 and 500 °C.

The CEC of the stevensite clay material is 42.5 cmol(+)/kg and the BET-specific surface area is 238 m<sup>2</sup>/g. Both properties were mostly conserved when treated hydrothermally and under hermetic conditions with steam up to 200 °C [21]. In general, a decrease in both properties is observed with increasing thermal treatment.

After the enzyme immobilization on the pellets, those previous characteristics changed. The BET-specific surface area in the sample treated at 200 °C decreases to 94.6 ± 0.2 m<sup>2</sup>/g, which is around half of the area of the initial pellets.

Treatment at 200 °C was initially preferred over higher temperatures due to the higher CEC and surface area and lower energy consumption required to produce the pellets. However, the physical cohesion of the pellets immersed in water had stronger results with the increasing temperatures when they were shaken. Therefore, subsequent experiments performed on reactive transport were performed with selected pellets, either treated 200 °C (as representative of low-temperature treatment) or 500 °C (representative of high-temperature treatment). Finally, for the experiments performed with the immobilized enzyme on the stevensite pellets, the material treated at 300 °C was used, as it presented better enzymatic fixation than at 200 °C (further explanation is given below).

### 3.2. Determination of the Hydrodynamic Parameters of the Geofilter by Non-Reactive Transport

In order to obtain confidence on the homogeneity of the porous filter, considering stable hydrodynamic conditions, it was necessary to repeat and compare different transport experiments.

To determine the hydrodynamic parameters, three replicates of the non-reactive transport experiments using  $\text{NaNO}_3$  were performed with pellets treated at 200 °C. The anionic transport was studied, as nitrate is not adsorbed by the stevensite clay (Figure 4).

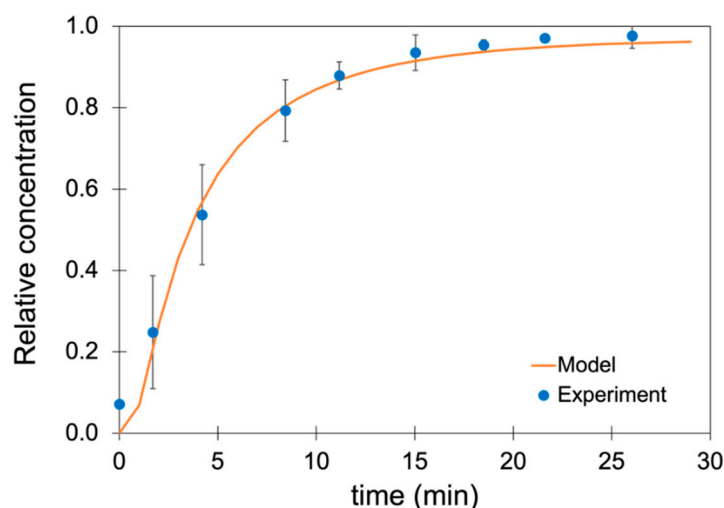


**Figure 4.** Non-reactive transport of  $\text{NO}_3^-$  through the geofilter and curve fitting with STANMOD.

For the present fit, the retardation factor was adjusted to 1, as nitrate is considered non-reactive and no degradation was assumed. Thereafter, by the inverse method with STANMOD,  $v$  and  $D$  were determined as 0.38 and 0.43, respectively. Although larger errors are found at short term, the experimental data in the three replicates converge with the increasing time. The regression coefficient for the curve fitting is 0.99.

### 3.3. Reactive Transport of TC through the Geofilter

To illustrate the effect of the adsorption capacity of tetracycline as a function of the temperature treatment of the clay pellets, reactive transport experiments were carried out with pellets treated at 200 and 500 °C. These experiments were performed with a constant concentration of TC solution of 1 g/L injected through the filter. The breakthrough curves are presented in Figure 5. Experiments were ended once a plateau of the relative concentration was reached. It can be observed that slightly higher adsorption is obtained with the pellets treated at 200 °C, but at long term, over 170 min, both experiments reach the same plateau. Assuming that the dispersion coefficient and the porewater velocity obtained by the non-reactive experiments are valid under reactive conditions, the retardation and degradation factors are calculated with STANMOD by the inverse curve fitting of the experimental data. A retardation factor of 8.43, a degradation factor of 0.07 and a regression coefficient of 0.99 were obtained at both temperatures, 200 and 500 °C. The retardation factor is far above 1, indicating significant adsorption of TC on the stevensite pellets. The low positive value for the degradation factor indicates insignificant degradation, although complexation reactions on the surface of the stevensite clay are not discarded, preventing TC degradation.

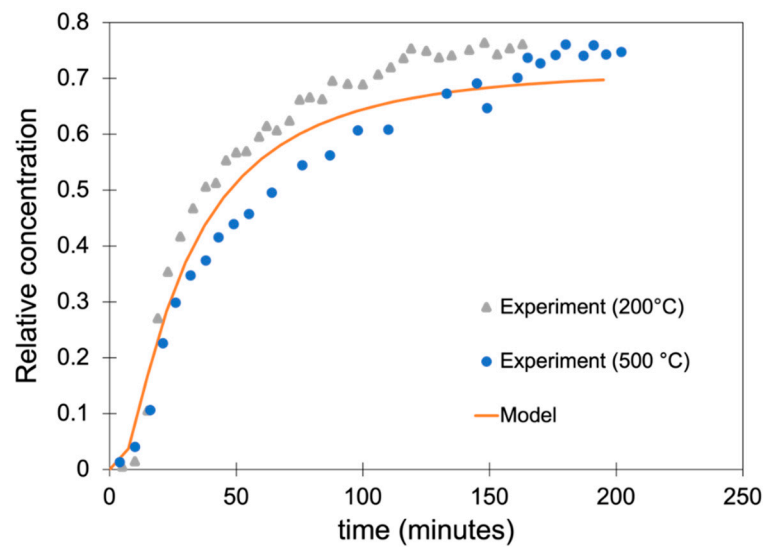


**Figure 5.** Breakthrough curve of 1 g/L TC solution through the geofilter prepared with stevensite treated at 200 °C (grey triangles) and 500 °C (blue circles). STANMOD curve fitting is presented by the orange line.

### 3.4. Desorption of TC

In the perspective of a real case scenario, the filter should exhibit desorption capacity, so that once the filter is saturated, it could be renovated by desorption of the organic contaminants by the outflow of a new inflow solution with capacity to exchange adsorption positions on the stevensite, recovering the filter in similar conditions as in its initial state and collecting the contaminant in a short time stage. A 1 M  $\text{Mg}(\text{NO}_3)_2$  solution at pH = 2 was used for desorption due to the high affinity of  $\text{Mg}^{2+}$  to the cation exchange sites in stevensite (Figure 6).

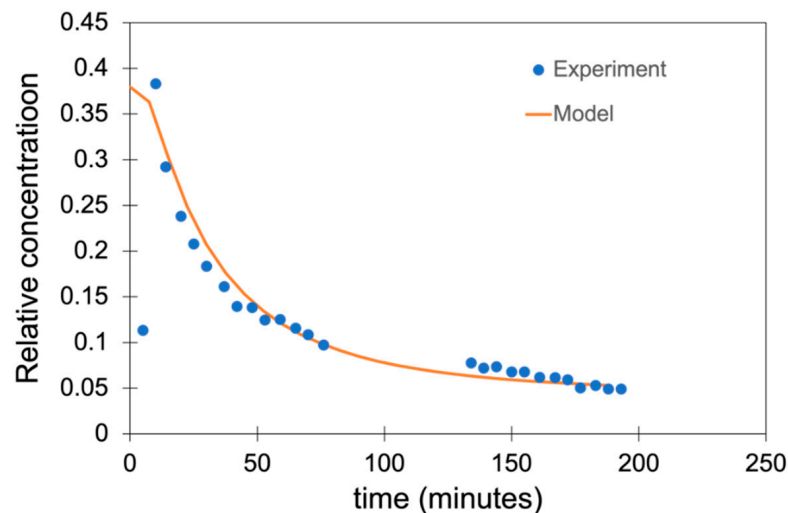


**Figure 6.** Desorption breakthrough curve of tetracycline with 1 M magnesium nitrate in a geofilter prepared with stevensite pellets treated at 200 °C, previously saturated with 1 g/L TC. Blue dots indicate the experimental data and the orange line the model fitting with STANMOD.

A relatively fast desorption can be observed as, after two hours, a negligible concentration of TC remains in the filter. Then, a new transport experiment could be carried out. All thermally treated stevensite clays conserve their sorption/desorption capacity.

### 3.5. Transports with Different Organic Molecules

In order to evaluate the adsorption capacity of the stevensite pellets, transport experiments were performed with 3 different organic molecules: TC (cationic at pH < 3.3, polar), eriochrome cyanine R (ECR; anionic at neutral pH, polar) and 4-nitrophenol (NP; neutral at controlled pH, weakly polar).

The 3 injected concentrations are 100 mg L<sup>-1</sup>.

The transport of ECR admitted a retardation factor of 1.67, calculated by STANMOD. Anions and anionic molecules, in general, are poorly retained by clays. However, a certain reactivity was observed in this assay.

Significant retention of the neutral organic molecule NP indicated that ion exchange was not the only mechanism of adsorption on the clay surface, presumably due to the action of van der Waals interaction with the polar surface of the clay. The retardation factor calculated by STANMOD for NP was 3.04.

In contrast, the cationic form of TC was clearly highly efficiently retained by the geofilter. A high retardation factor of 52.8 indicates that the stevensite pellets are good candidates to retain cationic molecules. Comparing the *R* with an injected TC solution at 100 and 1000 ppm, it can be deduced that the retardation factor also depends on the concentration of the inflow solution. More importantly, a positive and relatively high factor of degradation of 0.13 has been required by STANMOD to fit the experimental curve. Although not shown in Figure 7, the three curves fitted with STANMOD exhibited regression coefficients higher than 0.996.

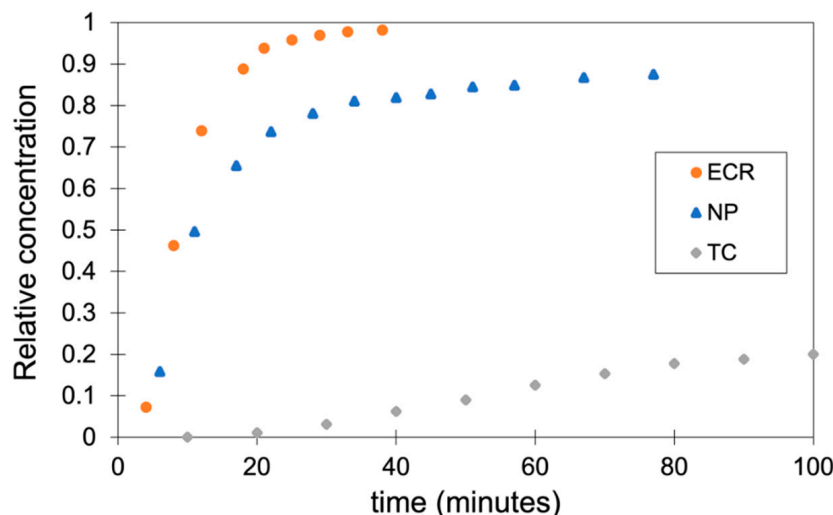


Figure 7. Breakthrough curves of ECR (orange), NP (blue) and TC (grey).

### 3.6. Transport with Enzymes Immobilized on the Stevensite Clay

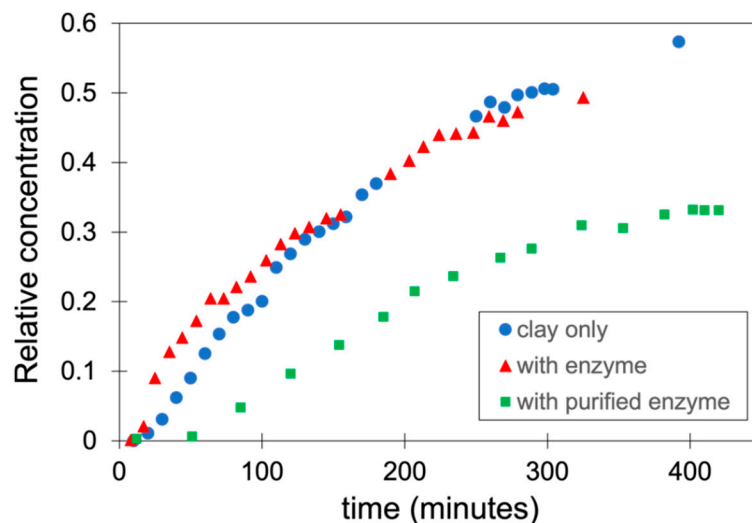
Once the process of enzyme fixation was completed, the laccase activity of the stevensite clay—immobilized laccase pellets was confirmed by visual observation of the oxidation of 2,6-dimethoxyphenol. The laccase activity of the stevensite clay—immobilized laccase pellets cannot be quantified because the oxidation product was adsorbed on pellets. The results of the test are shown in Table 1.

Table 1. Visual observation of the laccase activity of stevensite clay—immobilized laccase pellets.

Buffer + DMP = (1)	(1) + Pellets without Enzyme	(1) + Pellets with Enzyme	(1) + Enzyme Solution
uncolored solution X	uncolored solution uncolored clay	colored solution colored clay	colored solution X

For the transport experiment performed with the biogeofilter, only pellets treated at lower temperature were studied. However, the pellets treated at 200 °C presented

dispersion of aggregates in solution during the process of enzymatic fixation. Therefore, it was chosen to work with the pellets treated at 300 °C because they resist the enzymatic fixation process better. Transport experiments of a solution of TC were performed at 100 mg L<sup>-1</sup> through the filter with the two kinds of enzymes immobilized on it, purified under laboratory conditions and commercial (Figure 8).



**Figure 8.** Breakthrough curve of TC in the biogeofilter made with thermally treated clay at 300 °C (blue), with addition of commercial solution form of enzyme, immobilized on the surface of the stevensite clay (red), and with purified enzyme in laboratory conditions, also immobilized on the surface of the stevensite clay (green).

The degradation of TC with the purified enzyme was significant. The concentration was nearly one third of the initial concentration after 360 min of transport. This significant degradation observed in the filter with the purified enzyme can also be illustrated by a higher degradation factor obtained with STANMOD, compared to the filter without enzyme and with non-purified enzyme, equal to 0.29 ( $r^2 = 0.998$ ), 0.133 ( $r^2 = 0.99$ ) and 0.172 ( $r^2 = 0.998$ ), respectively.

The retardation factor was also higher in the experiment with the purified enzyme. A value of 103.3 ( $r^2 = 0.998$ ) was obtained with STANMOD for this experiment, while for the transport experiment without enzyme and with the non-purified enzyme, the retardation factor was 52.8 ( $r^2 = 0.99$ ) and 47 ( $r^2 = 0.998$ ), respectively.

Reactive transport with 3 different concentrations of TC injected solution—200, 100 and 50 mg L<sup>-1</sup>—were carried out with a filter, with and without enzyme. The area ratios were calculated once plateaus were reached, after 400 min (Table 2).

**Table 2.** Area ratio and degradation percentage as a function of the concentration of the injected solution.

$C_i$ (mg L <sup>-1</sup> )	A (with Enzyme)/A (without Enzyme)	Degradation (%)
200	0.96	4
100	0.53	47
50	0.42	58

During the transport, the TC was not totally degraded, but there were many degradation intermediates going out of the filter. On the UV-visible spectrum performed after HPLC separation, seven products of degradation can be detected after the transport, but their identification lies out of the scope of the present study.

## 4. Discussion

### 4.1. Hydrothermal Treatment

The hydrothermal treatment allows the modification of manufactured stevensite clay pellets, with physical cohesion maintained within the filter and, consequently, inducing a better longevity in the filter material. All the results show that the stevensite pellets still maintain large adsorption capacity. Considering a TC concentration of 1 g/L, after 3 h of transport, the outflow concentration is about 60% of the initial concentration using a filter manufactured with commercial powder stevensite [20]. Under the same experimental conditions, the outflow concentration is about 70% with the stevensite pellets in the current work.

The choice of the temperature of the thermal treatment has no significant effect on the breakthrough curve of the TC transport. The CEC, as well as the specific surface area, vary according to the heat treatment applied. Samples treated at lower temperature, 200 and 300 °C, have higher CEC and specific surface area than those treated at higher temperature, 400 and 500 °C. However, numerical values for both properties remain at the same order of magnitude and, thus, have little effect on the reactive transport. Therefore, the use of a low-temperature treatment (200 °C or 300 °C) was preferred because of the lower energy consumption. Samples treated at 300 °C resisted the enzymatic immobilization process, while those at 200 °C disperse. Hence, it is recommended to manufacture the stevensite pellets after treatment at 300 °C (as representative of low-temperature treatment) to make a biogeofilter with enzymes immobilized on the clay.

### 4.2. Interpretation of Transport Results

It can be observed that the breakthrough curves always followed the same tendency. A first increase of the relative concentration with a quasi-linear behaviour, then the relative concentration increased with a lower slope, reaching a long-time regime of very slow increase of relative concentration.

It can be assumed that the first part of the transport depends on the adsorption equilibrium of the TC on the clay. The second part is considered more dependent on the time, controlled by kinetics, for instance on diffusion of the solute inside the pellets, with the achievement of a relative high adsorption with time.

This interpretation is supported by the case of transport with the non-purified enzyme attached (Figure 9). It can be observed in the first part of the curve that TC was less absorbed in the presence of enzymes. This would agree with the presence of glutaraldehyde on exchange sites on the surface of the clay. Furthermore, in the second part of the curve, a lower increasing trend is witnessed. Degradation can be observed in a significant way. When the enzymatic activity was low, the adsorption of TC by the stevensite clay was the main phenomenon that varied the concentration of tetracycline. Whereas when the enzymatic activity was high (case of purified enzyme), degradation was a much more preponderant phenomenon, and it decreased the outflow of the TC concentration from the start of the transport.

With the CXTFIT model, either equilibrium transport or non-equilibrium can be modelled. The non-equilibrium situation can take several forms and interpretations. We decided to use the module with two sites of non-equilibrium chemical, which represents a situation of two different sorption sites on clays. The two sites model can be interpreted as a mobile and a stationary phase during transport. As observed in Figure 9, the experimental data was between the prediction by the one site equilibrium model and the two sites non equilibrium model.

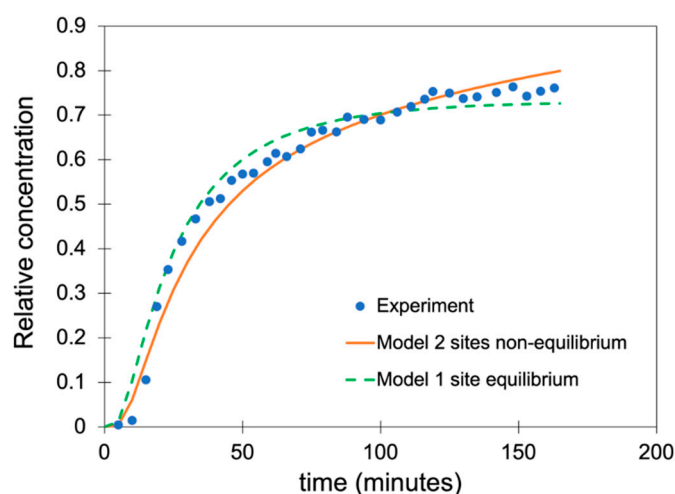


**Figure 9.** Comparison of the one site and two sites models to fit a  $1000 \text{ mg L}^{-1}$  TC transport experiment.

However, in the case of transport at lower concentrations, especially with the enzymes immobilized on the stevensite clay, the model produced a beta value very close to 1. This means that the situation was better simulated by the one site equilibrium model, thus the use of the non-equilibrium model was not necessary in this case.

#### 4.3. Determination of the Retardation Factor

Depending on the method of solving the retardation factor, very different results can be obtained [39]. Methods based on different analytical solutions, but applied to the same experimental data, will lead to different values for the retardation factor [40]. To be able to compare the different retardation factors, it is necessary that they were calculated with the same method.

The retardation factor was calculated by different theoretical methods for the transport experiment performed with  $1000 \text{ mg L}^{-1}$  of TC (Table 3).

**Table 3.** Estimation of the retardation factor with different methods for the transport experiment performed with  $1000 \text{ mg L}^{-1}$  of initial TC concentration.

Method	Retardation Factor
STANMOD	8.34
Moment method	4.56
Velocity ratio	7.73
Langmuir	2.66

The retardation factor depends on the concentration of the injected solution. To make predictions at low concentration, it is necessary to find a relation between the retardation factor and the concentration injected. By means of the experiments performed in the present study with TC solutions of 50, 100, 200 and  $1000 \text{ mg L}^{-1}$ , the mathematical function  $R = 156.26c_i^{-1.615}$  ( $r^2 = 0.92$ ) has been obtained to relate the normalized retardation factor ( $R$ ) as a function of the TC concentration injected ( $c_i$ ).

Therefore, using this mathematical function to predict the retardation factor for low concentrations, values of 156 and 644 are found for inflow concentrations of  $1 \text{ mg L}^{-1}$  and  $1 \mu\text{g L}^{-1}$ , respectively.

#### 4.4. Determination of the Degradation Factor

Now, assuming the same calculation as for the values in Table 2, the area ratio increases with the concentration, following exponential Equation (7):

$$A \text{ ratio} = 0.315e^{0.0055C_i} \quad (r_2 = 0.998) \quad (7)$$

For low concentrations, the *A ratio* might be considered independent of the concentration and equal to 0.315. Low degradation percentages can be assumed in aqueous solutions containing only TC, but in complex matrices solutions, this assumption would probably not be valid. Therefore, the degradation for low concentrations can be predicted (Table 4). As for the data in Table 2, the area ratios were calculated after 400 min.

**Table 4.** Prediction of degradation for low concentrations.

$C_i$ (mg L <sup>-1</sup> )	A (with Enzyme)/A (without Enzyme)	Degradation (%)
1	0.316	68.3
0.1	0.315	68.5

#### 4.5. Direct Method Approach for a Real Case Scenario

For technical reasons, we were not able to carry out experiments with concentrations lower than 50 mg L<sup>-1</sup>. In addition to much longer experimental times, the fast track of the outflow concentration during the run of experiments could not have been possible with the available equipment. However, the actual concentrations of antibiotics in the wastewater is in the range of µg L<sup>-1</sup>.

Making use of the above estimations performed in the present work, we have performed an exercise to predict the efficiency of the biogeofilter with TC concentration of 100 µg L<sup>-1</sup>. To do that, we use a direct approach with the STANMOD program with the following parameters:

$v = 0.38$  cm/min;  $D = 0.43$  cm<sup>2</sup>/min, estimated with the same proportion of mixture clay:sand 1:1; hydrodynamic parameters are approximately conserved. The values for  $R$  and  $\mu$  were estimated in the previous Tables 3 and 4. The results of the present estimation are shown in Figure 10 and Table 5.

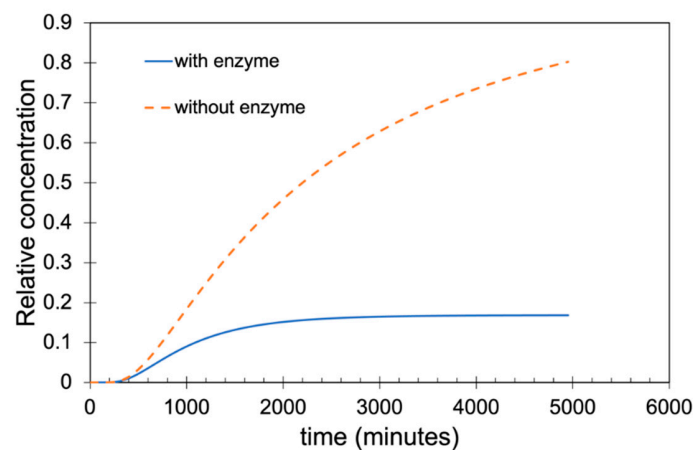


**Figure 10.** Predicted breakthrough curve for an inflow TC concentration of 100 µg L<sup>-1</sup>.

**Table 5.** Hydrodynamic parameters chosen for the prediction at 100 µg L<sup>-1</sup>.

$v$	$D$	$R$	$\mu$
0.38	0.43	644	0.68

The projection shown in Figure 10 indicates that retention and degradation of TC in the biogeofilter is very efficient, working continuously for 3.5 days. A plateau is reached at around 0.15 times the initial concentration (15 µg L<sup>-1</sup>), indicating a long lifespan of the filter. Hence, 85% of the initial concentration can be retrieved with only 4.5 g of stevensite treating nearly 6 L of TC solution, therefore accounting for 1.3 m<sup>3</sup>/kg.

These estimated calculations are based on a solution containing only TC, however. In a real case scenario, either for irrigation systems or for additional water treatment in WWTP,

the water matrix will be rich in organic and inorganic compounds that will compete and probably hinder the performance of the biogeofilter. Although the analytical identification and quantification of TC might be difficult, further experimental studies should be focused on the evaluation of the performance of the biogeofilter in complex matrices, simulating contaminated waters.

The capacity for desorption is also an important feature in the biogeofilter if it is escalated to large scale. As in the study by Fernández et al. [20] for a geofilter made with a mixture of stevensite powder and quartz sand, the present study shows good desorption capacity for the geofilter made with stevensite pellets and quartz sand. In both cases, desorption has taken place fast, recovering mostly all adsorbed TC and regenerating the cation exchange positions of the stevensite by  $Mg^{2+}$ . Further studies should also be focused on the evaluation of the desorption capacity of the biogeofilter.

#### 4.6. Filter Length

In order to lower the output concentration, it is possible to increase the filter length. STANMOD modelling by direct method can be done by changing the filter length and keeping the other parameters constant (Figure 11).

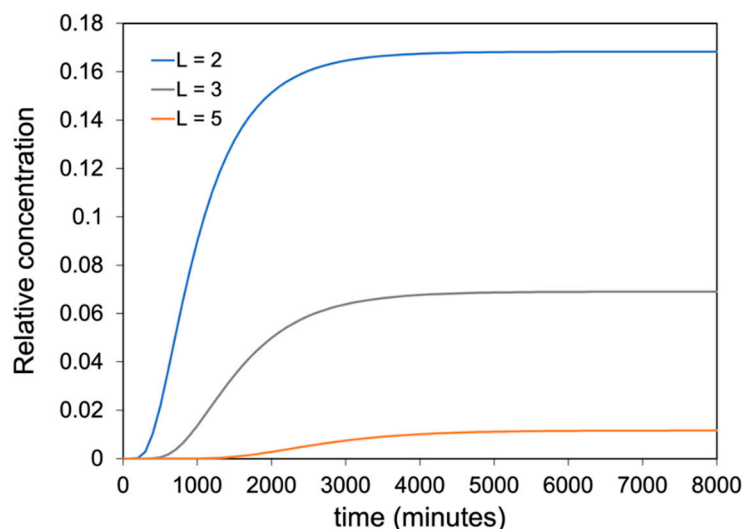


**Figure 11.** Modelling of breakthrough curve with different filter lengths.

It can be observed in Figure 11 that the longer the filter is, the lower the final output concentration achieved. Assuming a 5 cm length filter with 1 cm radius, 11.25 g of stevensite clay will be required to retrieve 99% of 6 L of TC. That is explained by the increase of the residence time of the reactant in the filter, thus with the same kinetic model, degradation is much higher.

#### 4.7. Large Scale Prediction

In all previous tests, the flow rate was imposed at  $1 \text{ mL min}^{-1}$ , which results in a pore linear velocity of  $0.38 \text{ cm min}^{-1}$ . With 4.5 g of clay in a 1:1 mixture (clay:sand), the TC concentration at the outflow is 16% of the initial concentration for a filter of 2 cm length.

If constant porosity is assumed and 1000 times higher volume is to be processed, 1000 times more mass of clay material is required. Therefore, to treat a flux of  $1 \text{ L min}^{-1}$  with an efficiency of 99%, 11.52 kg of stevensite pellets would be needed, with a filter of 5 cm length and 32 cm of radius.

Finally, the predictions considered in the present study are based on hydrodynamic properties calculated by the laboratory experiments that were performed at relatively low flow. Real case scenarios at large scale might require treating large volumes of solution. Therefore, the fluid flow might be higher, hence the interaction time between solutes and

the surface of the geo- or biogeofilter would decrease due to a kinetic effect that should be considered in further studies.

## 5. Conclusions

The manufacture of stevensite pellet solves the problem concerning the colloidal suspension of the powdered stevensite clay as a geofilter for organic pollutants such as antibiotics. The physicochemical characteristics of the geofilter manufactured with stevensite pellets maintain high adsorption capacity. Immobilization of enzymes on the filter is still possible.

The biogeofilter manufactured with stevensite pellets and laccase enzyme immobilized is able to significantly reduce the concentration of TC, as it has been observed in the transport experiments performed in laboratory conditions.

The efficiency of the biogeofilter at laboratory scale in cells of 2 cm of length and 1 cm of radius is high for the retention and degradation of TC and might lead to the development of a larger filter to be used for removing antibiotics in irrigation systems and wastewaters.

The model performed with the STANMOD code allowed calculation of hydrodynamic parameters by fitting the experimental data, was useful for the interpretation of the reaction mechanisms and predicted the performance of a real case scenario for a biogeofilter, considering a series of assumptions regarding filter dimensions and the inflow solution to be treated. The amount of clay and filter dimensions have been calculated theoretically for large-scale scenarios; however, further experiments will need to be conducted to verify the output of the models at lower concentrations, including large inflows and larger filter sizes. In addition, transport experiments performed with a more complex solution should be done in order to determine potential interferences for the adsorption and degradation of different solutes. We propose a well-known synthetic wastewater solution to continue the present study.

**Author Contributions:** Conceptualization, A.S., J.C. and R.F.; methodology, A.S., M.T., C.G.-D., A.O. and S.Z.; software, A.S.; validation, A.S., J.C. and R.F.; formal analysis, A.S., C.G.-D., J.C. and R.F.; investigation, A.S., J.C., A.I.R. and R.F.; resources, A.O., J.C., A.I.R. and R.F.; data curation, A.S.; writing—original draft preparation, A.S.; writing—review and editing, J.C., C.G.-D. and R.F.; visualization, A.S.; supervision, J.C. and R.F.; project administration, J.C. and E.E.; funding acquisition, J.C. and E.E. All authors have read and agreed to the published version of the manuscript.

**Funding:** This work was supported by the Spanish State Research Agency (Project PDC2021-120744-100). Adrien Saphy's stay in Madrid was funded by an Erasmus grant.

**Data Availability Statement:** The data presented in this study are available on request to the corresponding author.

**Acknowledgments:** We thank Tolsa for providing the Minclear N100™ stevensite clay. Adrien Saphy greatly thanks the staff of Universidad Autónoma de Madrid for hosting and helping him during his fruitful and rewarding internship. The authors thank the three anonymous reviewers that reviewed the manuscript for their helpful comments and suggestions.

**Conflicts of Interest:** The authors declare no conflict of interest.

## References

1. Homem, V.; Santos, L. Degradation and removal methods of antibiotics from aqueous matrices—A review. *J. Environ. Manag.* **2011**, *92*, 2304–2347. [[CrossRef](#)] [[PubMed](#)]
2. Sarmah, A.K.; Meyer, M.; Boxall, A.B. A global perspective on the use, sales, exposure pathways, occurrence, fate and effects of veterinary antibiotics (VAs) in the environment. *Chemosphere* **2006**, *65*, 725–759. [[CrossRef](#)]
3. Sabri, N.; van Holst, S.; Schmitt, H.; van der Zaan, B.; Gerritsen, H.; Rijnaarts, H.; Langenhoff, A. Fate of antibiotics and antibiotic resistance genes during conventional and additional treatment technologies in wastewater treatment plants. *Sci. Total. Environ.* **2020**, *741*, 140199. [[CrossRef](#)]
4. Sun, L.; Gao, C.; He, N.; Yang, B.; Duan, X.; Chen, T. The removal of antibiotic resistance genes in secondary effluent by the combined process of PAC-UF. *J. Environ. Sci. Health Part A* **2019**, *54*, 1075–1082. [[CrossRef](#)] [[PubMed](#)]

5. Frade, V.M.F.; Dias, M.; Teixeira, A.C.S.C.; Palma, M.S.A. Environmental contamination by fluoroquinolones. *Braz. J. Pharm. Sci.* **2014**, *50*, 41–54. [[CrossRef](#)]
6. Luo, Y.L.; Guo, W.S.; Ngo, H.H.; Nghiem, L.D.; Hai, F.I.; Zhang, J.; Liang, S.; Wang, X.C. A review on the occurrence of micropollutants in the aquatic environment and their fate and removal during wastewater treatment. *Sci. Total Environ.* **2014**, *473–474*, 619–641. [[CrossRef](#)]
7. Khorsandi, H.; Teymori, M.; Aghapour, A.A.; Jafari, S.J.; Taghipour, S.; Bargeshadi, R. Photodegradation of ceftriaxone in aqueous solution by using UVC and UVC/H<sub>2</sub>O<sub>2</sub> oxidation processes. *Appl. Water Sci.* **2019**, *9*, 81. [[CrossRef](#)]
8. Zhuang, Y.; Ren, H.; Geng, J.; Zhang, Y.; Zhang, Y.; Ding, L.; Xu, K. Inactivation of antibiotic resistance genes in municipal wastewater by chlorination, ultraviolet, and ozonation disinfection. *Environ. Sci. Pollut. Res.* **2015**, *22*, 7037–7044. [[CrossRef](#)]
9. Yu, F.; Li, Y.; Han, S.; Ma, J. Adsorptive removal of antibiotics from aqueous solution using carbon materials. *Chemosphere* **2016**, *153*, 365–385. [[CrossRef](#)]
10. Thiebault, T. Raw and modified clays and clay minerals for the removal of pharmaceutical products from aqueous solutions: State of the art and future perspectives. *Crit. Rev. Environ. Sci. Technol.* **2020**, *50*, 1451–1514. [[CrossRef](#)]
11. Christidis, G.E. Industrial Clays. In *Advances in the Characterization of Industrial Minerals*; Christidis, G.E., Ed.; European Mineralogical Union Notes in Mineralogy; The Mineralogical Society of Great Britain & Ireland: London, UK, 2011; Volume 9, pp. 341–414, ISBN 978-0-903056-28-1.
12. Aristilde, L.; Lanson, B.; Miéché-Brendlé, J.; Marichal, C.; Charlet, L. Enhanced interlayer trapping of a tetracycline antibiotic within montmorillonite layers in the presence of Ca and Mg. *J. Colloid Interface Sci.* **2016**, *464*, 153–159. [[CrossRef](#)] [[PubMed](#)]
13. Chang, P.-H.; Jean, J.-S.; Jiang, W.-T.; Li, Z. Mechanism of tetracycline sorption on rectorite. *Colloids Surfaces A Physicochem. Eng. Asp.* **2009**, *339*, 94–99. [[CrossRef](#)]
14. Figueroa, R.A.; Leonard, A.; MacKay, A.A. Modeling Tetracycline Antibiotic Sorption to Clays. *Environ. Sci. Technol.* **2003**, *38*, 476–483. [[CrossRef](#)] [[PubMed](#)]
15. Li, Z.; Schulz, L.; Ackley, C.; Fenske, N. Adsorption of tetracycline on kaolinite with pH-dependent surface charges. *J. Colloid Interface Sci.* **2010**, *351*, 254–260. [[CrossRef](#)] [[PubMed](#)]
16. Thiebault, T.; Boussafir, M.; Guégan, R.; Le Milbeau, C.; Le Forestier, L. Clayey–sand filter for the removal of pharmaceuticals from wastewater effluent: Percolation experiments. *Environ. Sci. Water Res. Technol.* **2016**, *2*, 529–538. [[CrossRef](#)]
17. Pozo, M.; Calvo, J.P. An Overview of Authigenic Magnesian Clays. *Minerals* **2018**, *8*, 520. [[CrossRef](#)]
18. Cuevas, J.; Pelayo, M.; Rivas, P.; Leguey, S. Characterization of Magnesium-Clays from the Neogene of the Madrid Basin and Their Potential as Backfilling and Sealing Material in High-Level Radioactive Waste Disposal. *Appl. Clay Sci.* **1993**, *7*, 383–406. [[CrossRef](#)]
19. Antón-Herrero, R.; García-Delgado, C.; Alonso-Izquierdo, M.; García-Rodríguez, G.; Cuevas, J.; Eymar, E. Comparative adsorption of tetracyclines on biochars and stevensite: Looking for the most effective adsorbent. *Appl. Clay Sci.* **2018**, *160*, 162–172. [[CrossRef](#)]
20. Fernández, R.; Ruiz, A.I.; García-Delgado, C.; González-Santamaría, D.E.; Antón-Herrero, R.; Yunta, F.; Poyo, C.; Hernández, A.; Eymar, E.; Cuevas, J. Stevensite-based geofilter for the retention of tetracycline from water. *Sci. Total Environ.* **2018**, *645*, 146–155. [[CrossRef](#)]
21. Tijero, M. Effect of Heat Treatment on Clay Granulates for the Construction of Filter Material for Emerging Pollutants. Master Thesis, Universidad Autónoma de Madrid, Madrid, Spain, 2022.
22. Polubesova, T.; Zadaka, D.; Groisman, L.; Nir, S. Water remediation by micelle–clay system: Case study for tetracycline and sulfonamide antibiotics. *Water Res.* **2006**, *40*, 2369–2374. [[CrossRef](#)]
23. Ghose, A.; Mitra, S. Spent waste from edible mushrooms offers innovative strategies for the remediation of persistent organic micropollutants: A review. *Environ. Pollut.* **2022**, *305*, 119285. [[CrossRef](#)] [[PubMed](#)]
24. Muñoz-Aguayo, J.; Lang, K.S.; LaPara, T.M.; González, G.; Singer, R.S. Evaluating the Effects of Chlortetracycline on the Proliferation of Antibiotic-Resistant Bacteria in a Simulated River Water Ecosystem. *Appl. Environ. Microbiol.* **2007**, *73*, 5421–5425. [[CrossRef](#)] [[PubMed](#)]
25. Rodriguez-Mozaz, S.; Vaz-Moreira, I.; Della Giustina, S.V.; Llorca, M.; Barceló, D.; Schubert, S.; Berendonk, T.U.; Michael-Kordatou, I.; Fatta-Kassinos, D.; Martinez, J.L.; et al. Antibiotic residues in final effluents of European wastewater treatment plants and their impact on the aquatic environment. *Environ. Int.* **2020**, *140*, 105733. [[CrossRef](#)] [[PubMed](#)]
26. ACD/ChemSketch Advanced Chemistry Development, Inc. (ACD/Labs), Toronto, ON, Canada. 2021. Available online: <https://www.acdlabs.com/products/chemsketch/> (accessed on 15 August 2022).
27. Couture, R.A. Rapid Increases in Permeability and Porosity of Bentonite-Sand Mixtures Due to Alteration by Water Vapor. *MRS Proc.* **1984**, *44*, 515. [[CrossRef](#)]
28. Heuser, M.; Weber, C.; Stanjek, H.; Chen, H.; Jordan, G.; Schmahl, W.W.; Natzeck, C. The interaction between bentonite and water vapor. I: Examination of physical and chemical properties. *Clays Clay Miner.* **2014**, *62*, 188–202. [[CrossRef](#)]
29. Meier, L.P.; Kahr, G. Determination of the Cation Exchange Capacity (CEC) of Clay Minerals Using the Complexes of Copper(II) Ion with Triethylenetetramine and Tetraethylenepentamine. *Clays Clay Miner.* **1999**, *47*, 386–388. [[CrossRef](#)]
30. García-Delgado, C.; Eymar, E.; Camacho-Arévalo, R.; Petruccioli, M.; Crognale, S.; D’Annibale, A. Degradation of tetracyclines and sulfonamides by stevensite- and biochar-immobilized laccase systems and impact on residual antibiotic activity. *J. Chem. Technol. Biotechnol.* **2018**, *93*, 3394–3409. [[CrossRef](#)]

31. Migneault, I.; Dartiguenave, C.; Bertrand, M.J.; Waldron, K.C. Glutaraldehyde: Behavior in aqueous solution, reaction with proteins, and application to enzyme crosslinking. *Biotechniques* **2004**, *37*, 790–802. [[CrossRef](#)]
32. Parker, J.C.; van Genuchten, M.T. Flux-Averaged and Volume-Averaged Concentrations in Continuum Approaches to Solute Transport. *Water Resour. Res.* **1984**, *20*, 866–872. [[CrossRef](#)]
33. Ogata, A.; Banks, R.B. *A Solution of the Differential Equation of Longitudinal Dispersion in Porous Media*; Professional Paper; U.S. Geological Survey: Washington, DC, USA, 1961; p. 7.
34. Chen, Z.L.; Feng, S.J.; Chen, H.X.; Peng, M.Q.; Li, Y.C.; Zhu, Z.W. Analytical Solution for Transport of Degradable Contaminant in Cut-off Wall and Aquifer. *Environ. Geotech.* **2022**, *in press*. [[CrossRef](#)]
35. Van Genuchten, M.T.; Šimunek, J.; Leij, F.J.; Toride, N.; Šejna, M. STANMOD: Model Use, Calibration, and Validation. *Trans. ASABE* **2012**, *55*, 1353–1366. [[CrossRef](#)]
36. Toride, N.; Leij, F.J.; van Genuchten, M.T. *The CXTFIT Code for Estimating Transport Parameters from Laboratory or Field Tracer Experiments*; U.S. Salinity Laboratory, U.S. Department of Agriculture: Riverside, California, CA, USA, 1995; p. 137.
37. Miralles, N.; Valderrama, C.; Casas, I.; Martínez, M.; Florido, A. Cadmium and Lead Removal from Aqueous Solution by Grape Stalk Wastes: Modeling of a Fixed-Bed Column. *J. Chem. Eng. Data* **2010**, *55*, 3548–3554. [[CrossRef](#)]
38. Nir, S.; Zadaka-Amir, D.; Kartaginer, A.; Gonen, Y. Simulation of adsorption and flow of pollutants in a column filter: Application to micelle–montmorillonite mixtures with sand. *Appl. Clay Sci.* **2012**, *67–68*, 134–140. [[CrossRef](#)]
39. Godoy, V.; Napa-García, G.F.; Zuquette, L. Determination of the sodium retardation factor using different methods: Analysis of their characteristics and impact on the solute movement prediction in a structured Brazilian soil. *Earth Sci. Res. J.* **2018**, *22*, 281–289. [[CrossRef](#)]
40. Van Genuchten, M.T.; Wierenga, P.J. Solute Dispersion Coefficients and Retardation Factors. In *Methods of Soil Analysis*; SSSA Book Series; John Wiley & Sons, Inc.: Hoboken, NJ, USA, 1986; pp. 1025–1054, ISBN 978-0-89118-864-3.